

Beam energy spread

Shanhong Chen
09 November 2021

Outline

□ Dr. Wang

- Layout about the mirror
- Energy spread
 - Motivation
 - Methods
 - Results
 - Summary & Questions

□ Dr. Duan

- orientation of the transverse polarization

横向极化方向

● 二、CEPC Z能区纵向极化方案:

➤ 纵向极化束流对撞:

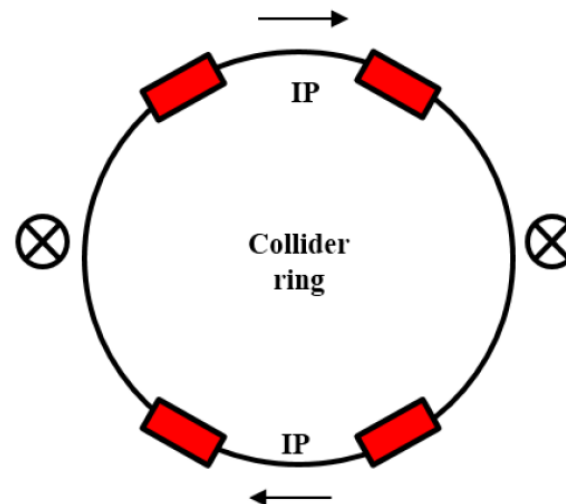
✓ 自旋旋转器:

自旋旋转器可以将极化方向从横向旋转为纵向，经过IP之后，再将极化方向旋转回来。

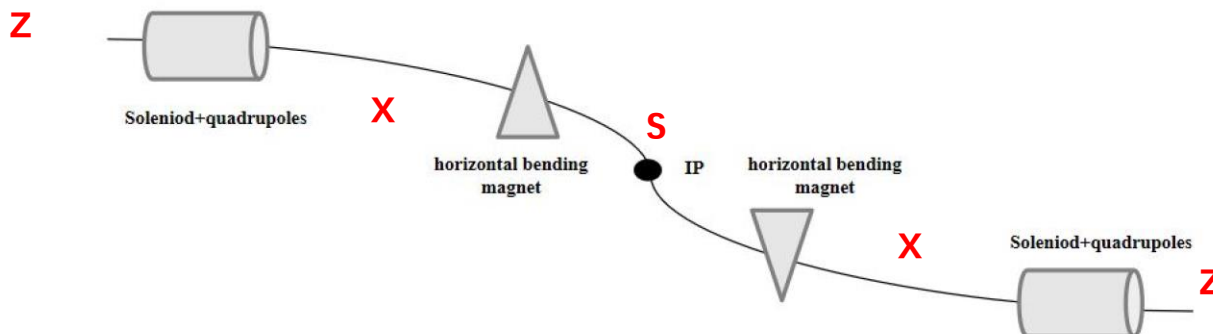
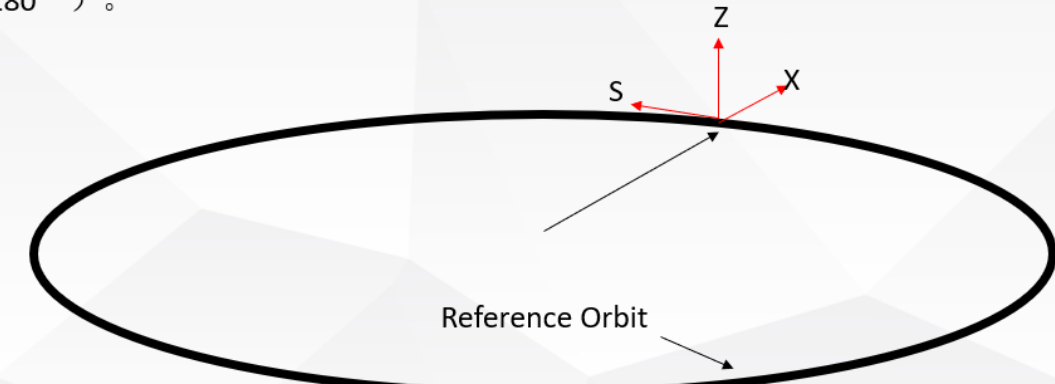
基于螺线管的自旋旋转器:

① 螺线管区域:

② 偏转磁铁区域: 水平偏转角度 0.015rad



- 我们常说的横向极化的方向指的是Z方向;
- 上次会议段哲师兄提出能否对X方向的极化进行测量;
- S方向是粒子运动方向，也就是我们说的纵向极化的方向
- 需要注意的是，以上提出的三种方向，分别对他们的反平行方向也是适用的（旋转 180° ）。



横向极化方向

$$d\sigma_0 = \frac{r_e^2}{\kappa^2(1+u)^3} \left(\kappa(1+(1+u)^2) - 4\frac{u}{\kappa}(1+u)(\kappa-u) \left[1 - \xi_\perp \cos(2(\varphi - \varphi_\perp)) \right] \right) du d\varphi,$$

$$d\sigma_{||} = \frac{\xi_\odot \zeta_\odot r_e^2}{\kappa^2(1+u)^3} u(u+2)(\kappa-2u) du d\varphi,$$

$$d\sigma_\perp = -\frac{\xi_\odot \zeta_\perp r_e^2}{\kappa^2(1+u)^3} 2u\sqrt{u(\kappa-u)} \cos(\varphi - \phi_\perp) du d\varphi.$$

Φ_\perp : transverse polarization azimuthal angle

$$\Phi_\perp \in [0, 2\pi]$$

- 横向1

$$\frac{d\sigma_\perp}{dxdy} = -\frac{\xi_\odot \zeta_\perp r_e^2}{(1+u)^3 \sqrt{1-x^2-y^2}} u \textcolor{red}{y}$$

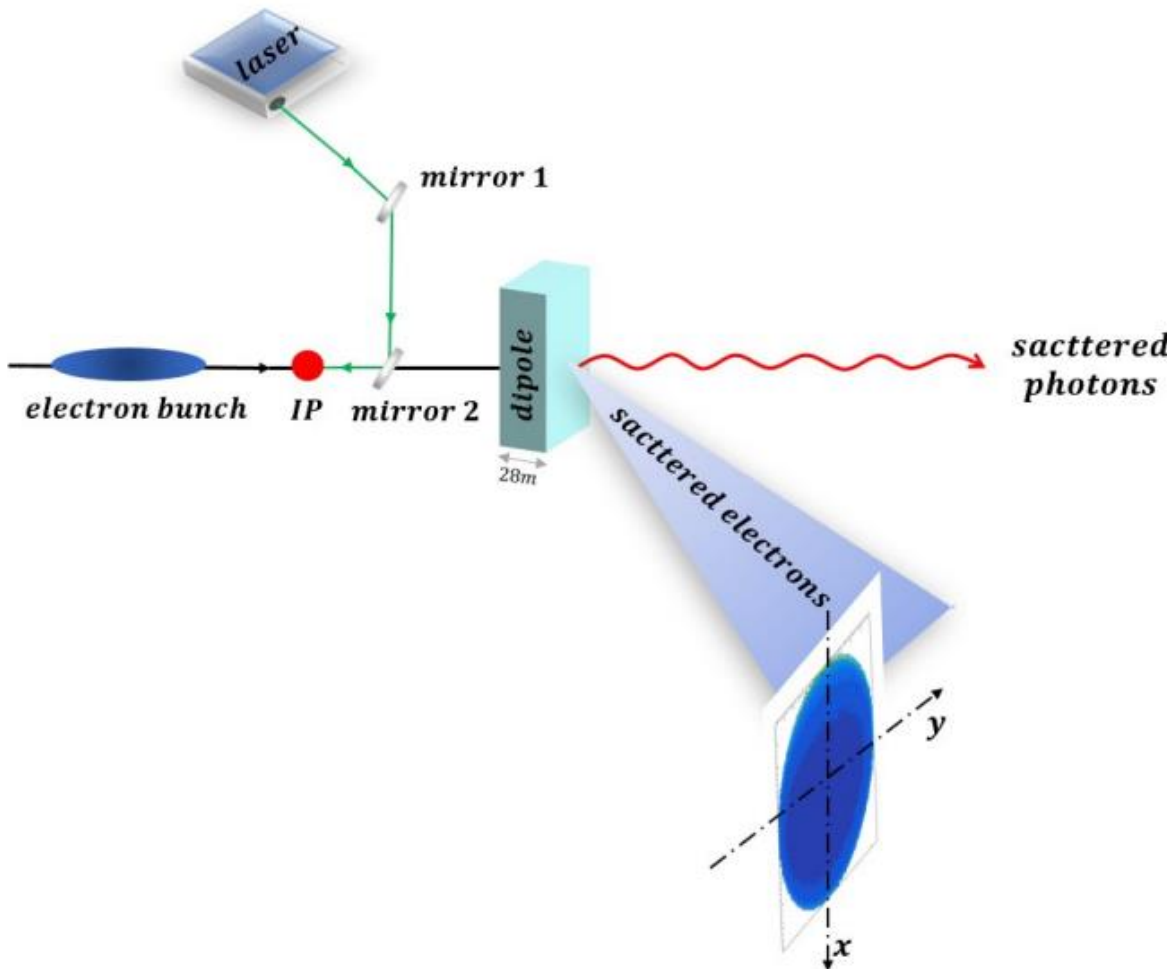
- 横向2

$$\frac{d\sigma_\perp}{dxdy} = -\frac{\xi_\odot \zeta_\perp r_e^2}{\kappa(1+u)^3 \sqrt{1-x^2-y^2}} 2u \sqrt{u(\kappa-u) - (\frac{\kappa \textcolor{red}{y}}{2})^2}$$

Transverse polarization of e^+/e^- beam influence the distribution on $\textcolor{red}{Y}\textcolor{red}{e}$ axis of scattered electrons.

2. **Background sources** need to be evaluated in the design of the polarimeter, e.g. from physical processes resulting in beam particle loss in the area close to the polarimeter, such as scattering on beam-gas molecules and on thermal photons, as well as from electron-positron interactions at the main IP with very small transverse momentum exchange;
3. Whether the beam polarisation should be measured upstream or downstream of the IP, or both, should be clarified. This might depend on the background conditions upstream and downstream, and on the capacity to evaluate beam-beam depolarisation effects using simulations for reliably extrapolating the foreseen polarisation measurements to the IP.

• Layout about the mirror



- 镜子尺寸：厘米量级
- 散射粒子和主束如果要区分成厘米量级的话，也得是漂移几百公里；所以主束一定得通过镜子，放在磁场前和磁场后是一样的效果；
- 唯一的补偿：我们的mirrow2是一个可以拉伸的装置，测量的话放进去，不测的话拉出来；
- 方案2：激光和电子90度对撞；90度进，90度出。物理要改， $\alpha=180/2 = 90^\circ$ ；意味着截面变小，意味着更长的取数时间。

Beam energy spread

- Motivation
- Requirement
- Methods
- Discussions

The motivation

- Essential requirement of experimental program is a stability of the collider parameters, including the beam energy spread of electron and positron beam[1].
- Reduce significantly a systematical error in the experiment of $c - \tau$ lepton mass measurement[2] influence the reliable initial-state radiation(ISR) factor and detection efficiency in hadron pair production.
- The statistics accumulation time at given collider luminosity L and mass measurement accuracy is proportional to the energy spread cubed[3].

$$\sigma_{eff} \propto \frac{\Gamma}{\sigma_w} \sigma_0$$

Where, σ_{eff} measured “effective” cross section of production of a narrow resonance with its intrinsic width being much smaller than the collider energy spread; Γ is the resonance width; σ_0 is the particle production cross section; σ is the beam energy spread
Mass measurement accuracy:

$$\Delta M \propto \frac{\sigma_w}{\sqrt{N_{ev}}} \propto \frac{\sigma_w^{3/2}}{\sqrt{\Gamma \sigma_0 L}}$$

Therefore,

$$L \propto \frac{\sigma_w^3}{\Delta M^2 \sigma_0 \Gamma}$$

[1] Meshkov, Oleg I., et al. "Study of beam energy spread at the VEPP-4M." EPAC 2006-Contributions to the Proceedings. 2006.

[2] Kiselev, V. A., et al. "Comparison of the Methods for Beam Energy Spread Measurement at the VEPP-4M." APAC2007: 4th Asian Particle Accelerator conference. 2007.

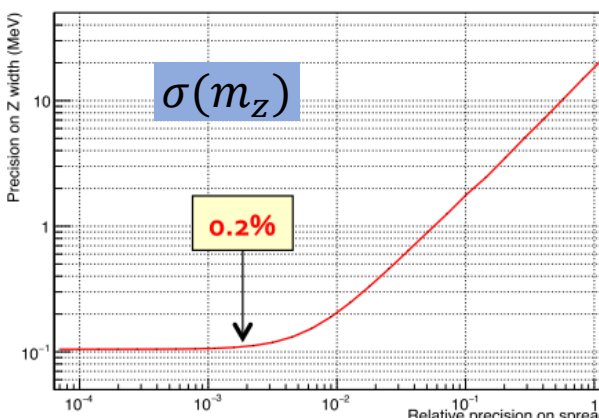
[3] Borin, V. M., et al. "Measurement of the VEPP-4M Collider Energy Spread in the Entire Energy Range." Physics of Particles and Nuclei Letters 17.3 (2020): 332-342.

Requirement

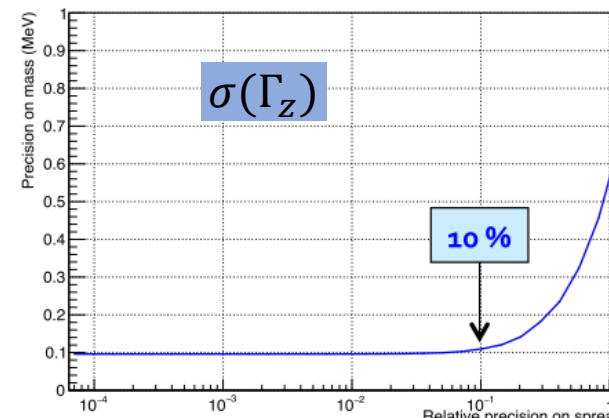
➤ FCC-ee Polarization Workshop (Patrick Janot)

□ We need an external measurement of the beam energy spread

- ◆ The precisions on m_Z , Γ_Z , and σ_o depend on the precision of this measurement



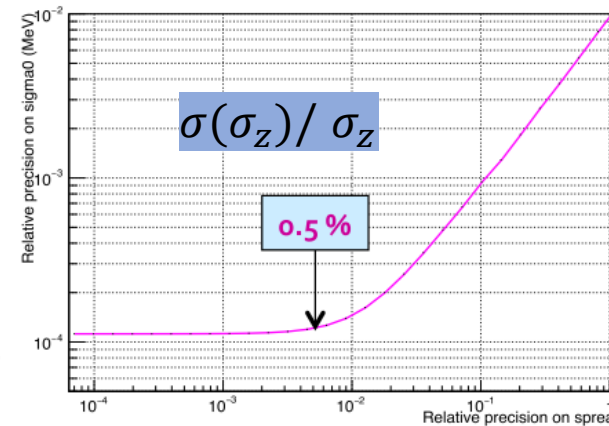
- Relative precision of 0.2% required !
 - Challenging beam instrumentation
 - See next talk ?
- ◆ Can we help with collision data ?



□ Targets set in the TLEP paper

- Precision on the Z width: 100keV
- Precision on the Z mass: 100keV
- Precision on the peak cross section: 10^{-4}

□ Relative precision of 0.2% required.



Techniques

➤ 1. Chromatic dependence of vertical betatron oscillations ν_y

在束流回旋振荡谱中，存储环的色度会导致同步带峰出现，也就是回旋频率谱上会出现多个峰。这些峰的幅度与能散有关，可以测它们的相对幅度来得到能散。

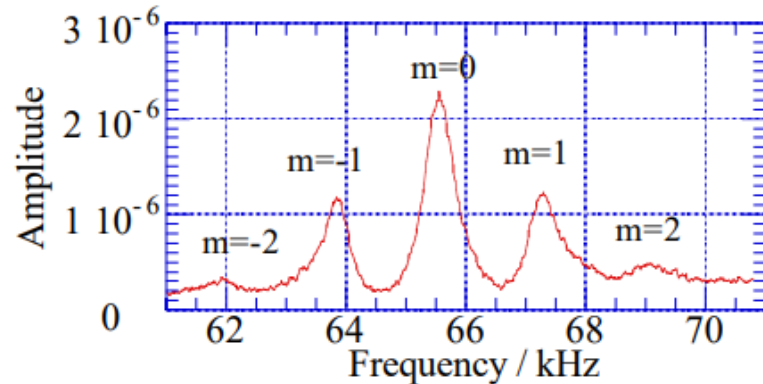


Figure 1: Example of measured frequency response of vertical betatron motion of a beam in the SPring-8 storage ring. Chromaticity is 8 and synchrotron frequency is 1.63kHz.

Finite **chromaticity** of storage rings produces the **synchrotron sideband peaks** in frequency response of betatron motion and **reduces the main peak height**.

Nakamura, T., et al. "Chromaticity for energy spread measurement and for cure of transverse multi-bunch instability in the SPRING-8 storage ring." *PACS2001. Proceedings of the 2001 Particle Accelerator Conference (Cat. No. 01CH37268)*. Vol. 3. IEEE, 2001.

- The amplitude of the central betatron peak and the synchrotron satellites are:

$$R_m(y) = \frac{1}{y^2} \int_0^\infty J_m^2(x) e^{-x^2/2y^2} x dx$$
$$y = \left(\frac{w_\beta \alpha}{w_s} + \frac{w_o C_y}{w_s} \right) \sigma_E$$

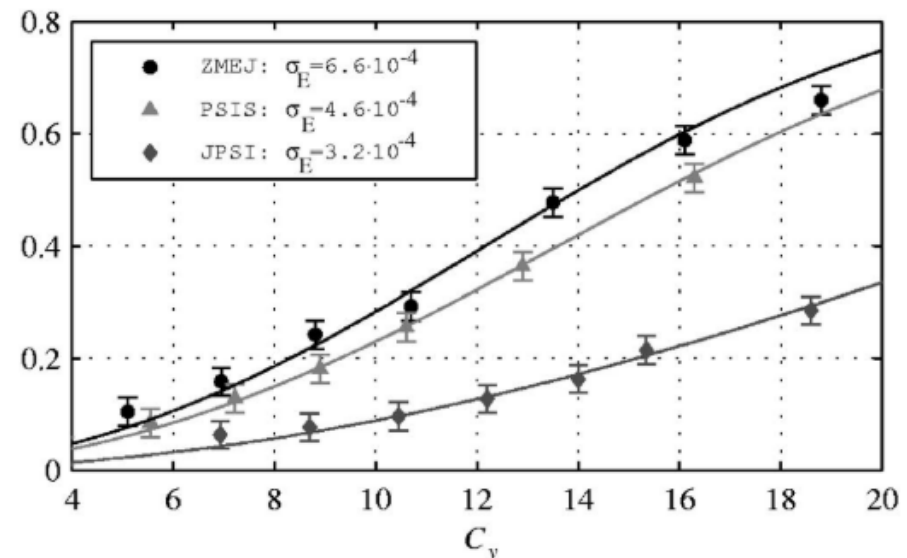


FIG. 13. Ratio of R_1/R_0 for a set of the VEPP-4M operation modes. Experimental points and theoretical curves are shown.

Techniques

➤ 2. Radial and longitudinal beam dimensions dependence of energy spread

➤ Principle

- Radial and longitudinal beam dimensions σ_{xz} were taken to determine current dependence of the beam energy spread.

$$\sigma_i^2 = \beta_i \varepsilon_i + (\eta_i \sigma_w)^2$$

ε_i : beam emittance

σ_w : beam energy spread

η_i : 色散函数?

➤ Applications

- ✓ 对HEPS Booster不同模式以及升能过程的束流状态进行观测：发射度与能散随着能量提高而降低，降至最低后，达到平衡。
- ✓ VEPP-4M

➤ Measure beam dimensions

基于同步辐射光的束流尺寸测量方法：1. 同步光成像法；2. 空间干涉法；3. X射线小孔成像法；4. KB镜聚焦成像法。采用同步光成像法，通过对束流光源点进行成像可直接观测束流状态，再对成像光斑进行高斯拟合可得到束流水平及垂直尺寸。

Techniques

➤ 3. Compton Back-Scattering

✓ BEPC、VEPP-4M

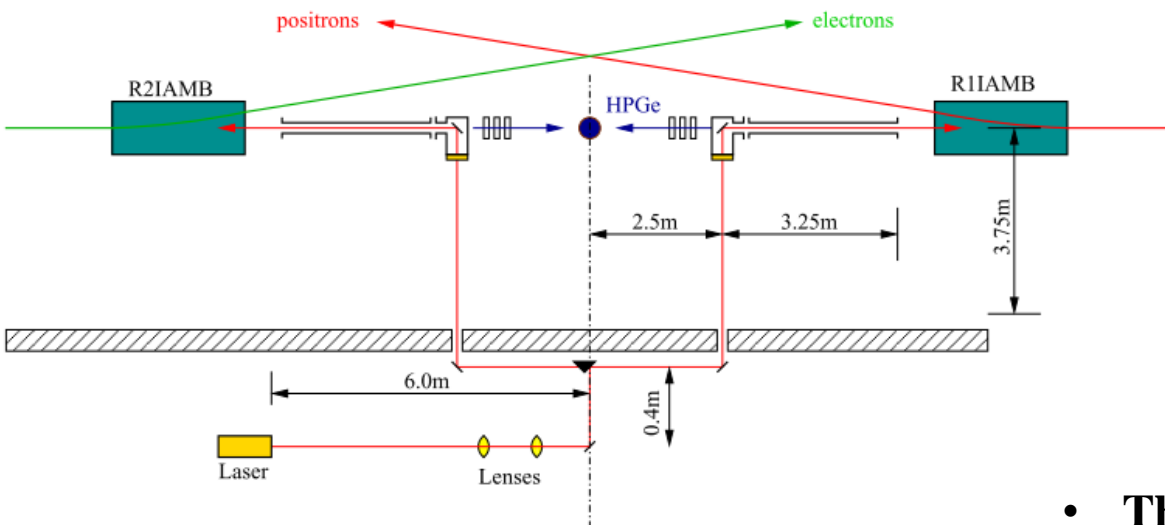
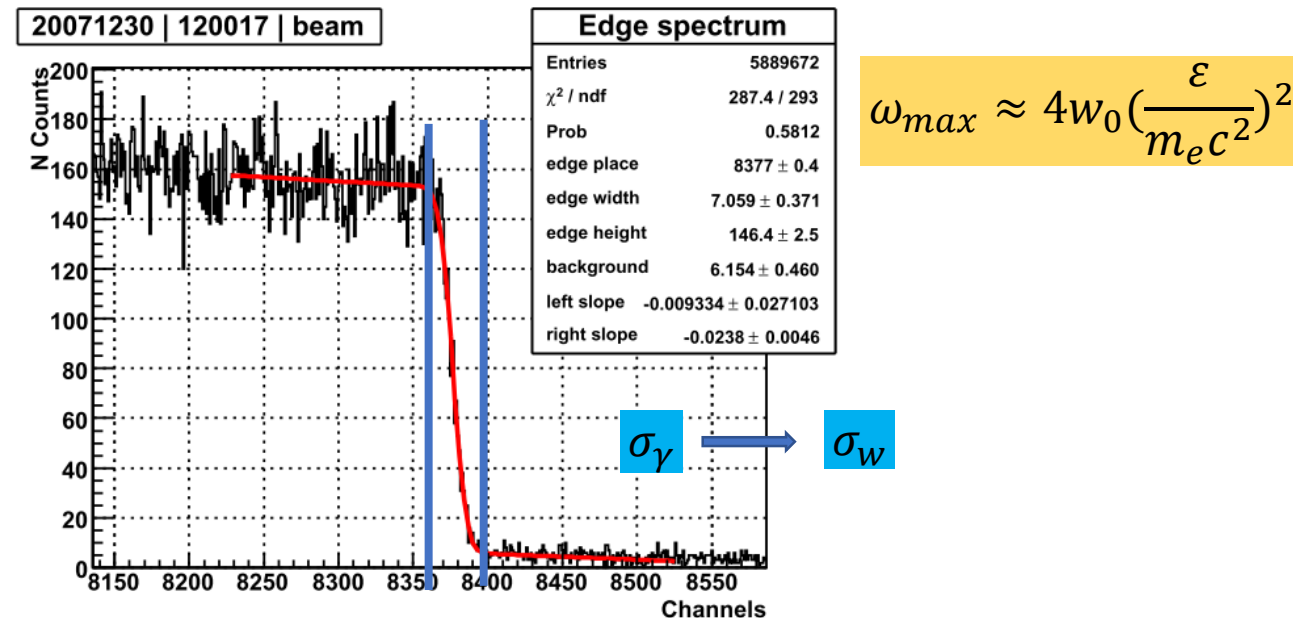


Figure 5: The apparatus layout at the BEPC-II.



- **The width of the edge** is mostly determined by the resolution of the photons detector and **the energy spread** in the electron beam

| | VEPP-4M | BEPC |
|---------------|--|---|
| LASER | Infrared laser with $\omega_0 = 0.117\text{eV}$ | Monochromatic laser with $\omega_0 = 0.12\text{eV}$ |
| Electron beam | Beam energy $\varepsilon = 1842\text{MeV}$ at ZMEJ mode | Beam energy $\varepsilon = 1842\text{MeV}$ |
| HPGe | Detector resolution 4×10^{-4} | Energy resolution 10^{-3} |
| Energy | $\delta\varepsilon/\varepsilon \leq 5 \times 10^{-5}$ statistical accuracy | $\delta\varepsilon/\varepsilon \leq 2 \times 10^{-5}$ |
| energy spread | $\delta E = 1.13 \pm 0.04\text{MeV}(3.5\%)$ | 6% |

$$\omega_{max} \approx 4w_0 \left(\frac{\varepsilon}{m_e c^2} \right)^2$$

Techniques

➤ 4. BEPCII

➤ Center-of-mass energy spread σ_E

- based on threshold truncation effect
- $\sigma_E = \sqrt{2}\sigma_B$

➤ Beam energy spread σ_B

- beam-constrained mass (MBC) spectra resolution.

Techniques

➤ The center-of-mass energy spread σ_E

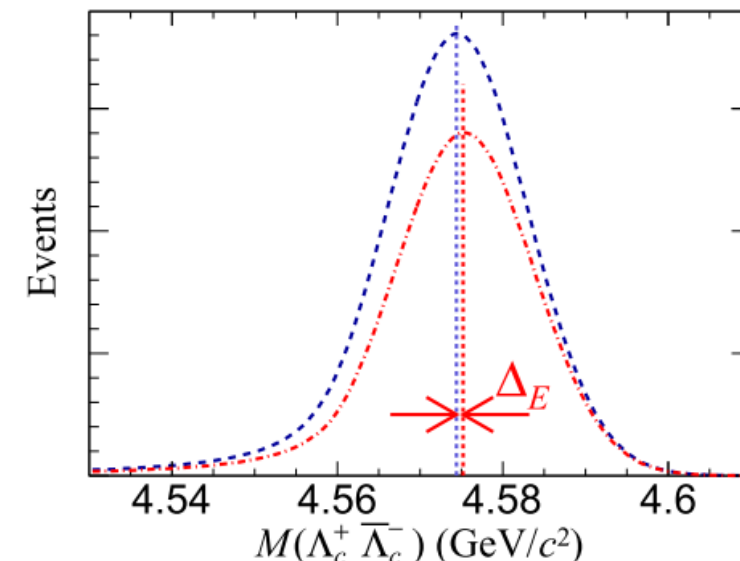
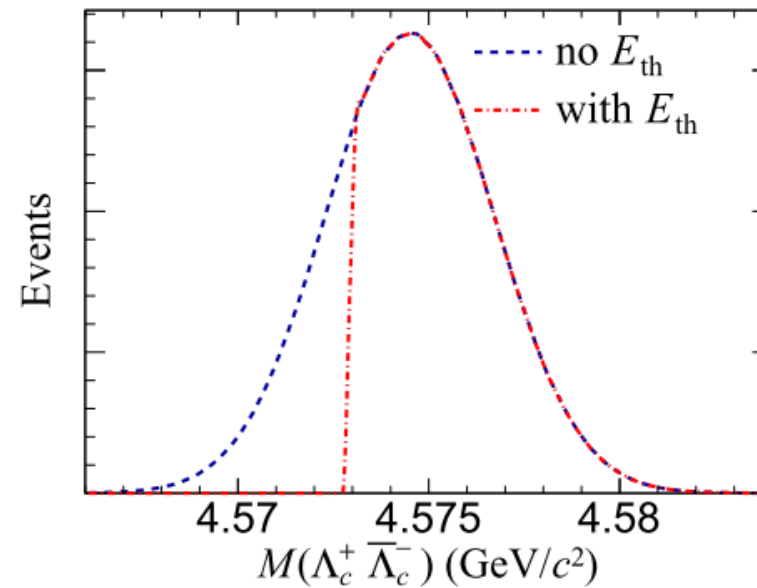
$$e^+ e^- \rightarrow X$$

$$e^+ e^- \rightarrow \Lambda_c^+ \bar{\Lambda}_c^-$$

- The c.m. energy is equal to the invariant mass of the final states X: $\sqrt{s} = M(X)$
- the reconstructed invariant mass tends to be higher than \sqrt{s} , due to the absence of some collisions below the production threshold caused by the energy spread.
- The observed invariant mass is expected to increase as the energy spread gets larger.
- $\Delta E = M(X) - \sqrt{s}$

- ✓ The distribution of $M(\Lambda_c^+ \bar{\Lambda}_c^-)$ **with (red)** and **without (blue)** **threshold truncation effect** before (left) and after (right) **detector reconstruction**.

- ✓ The larger detector resolution, the smaller ΔE

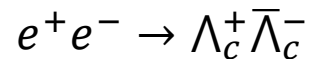
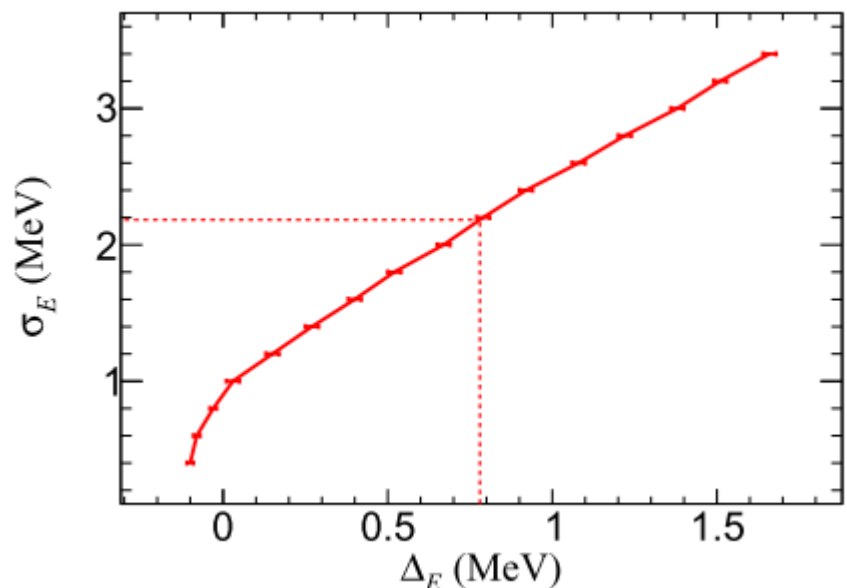


Techniques

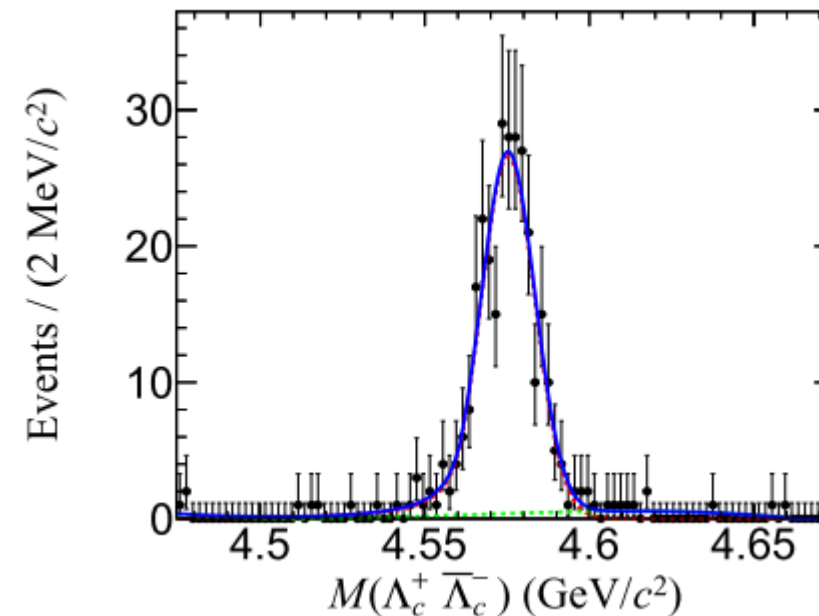
- The center-of-mass energy spread σ_E

The toy MC simulation:

$E = 4575\text{MeV}$ for different energy spread,
the relationship between ΔE and σ_E



- ✓ An example of Method results



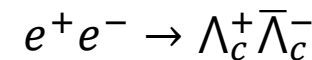
$$M(\Lambda_c^+\bar{\Lambda}_c^-) = 4575.28 \pm 0.55\text{MeV}$$

$$\Delta E = M(\Lambda_c^+\bar{\Lambda}_c^-) - \sqrt{s} = 0.78\text{MeV}$$

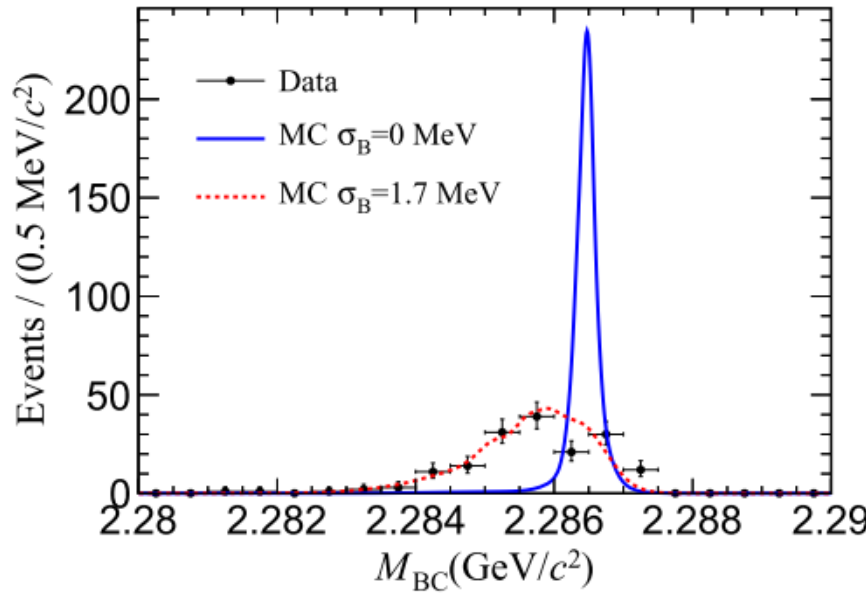
$$\sigma_E = 2.2 \pm 1.1\text{MeV}$$

Techniques

➤ Beam energy spread σ_B

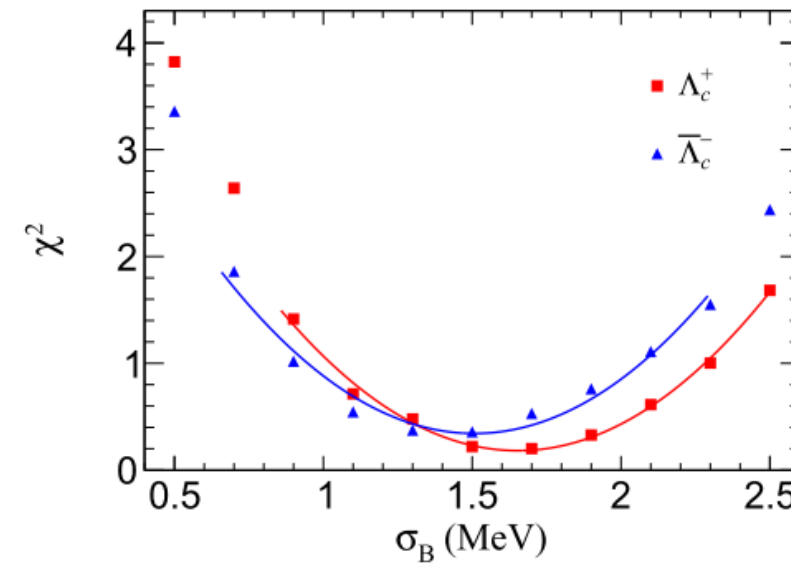


- The beam-constrained mass M is used to reflect the difference between data and MC simulations
- The beam energy is equal to the mass of Λ_c^+ or $\bar{\Lambda}_c^-$



M distribution fitted with signal shape obtained from pure signal simulation with (red dashed line) and without (blue solid line) beam energy spread at 4575MeV. The shapes are scaled by the number of events.

- Scan
- Set a series of σ_B , find the best fit result: χ^2 value



$\sigma(\sigma_B)$ is the half of width of $\chi^2 + 1$

Questions / remarks

- **Is the beam energy profile expected to be Gaussian ?**
 - ◆ In particular, is the beamstrahlung-induced spread expected to be Gaussian ?
 - ◆ Need to check with another shape (e.g., triangular, rectangular, same RMS)
- **Is the beam energy profile at least expected to be symmetric ?**
 - ◆ In particular, is the beamstrahlung-induced spread expected to be symmetric ?
 - ◆ If it is not symmetric, the effect on the masses will be larger
 - Need to check how much larger
 - And also predict the effect of such an asymmetry on the energy calibration
 - Need to check whether we can determine the actual shape with dimuon events
 - Require unfolding of ISR and angular resolution from $\sqrt{s'}$
 - Need some insights from beam instrumentation
- **Is the beam energy profile expected to be the same at the two IPs ?**
 - ◆ If not, can the difference be predicted from beam instrumentation ?
- **Check if electrons (and maybe taus) can be used too**
 - ◆ More difficult : electron bremstrahlung and tau decays affect the directions
- **Investigate methods to map the θ and ϕ resolutions in the tracker**
 - ◆ E.g., with other resonances decaying to $\mu^+\mu^-$ (ϕ , J/Ψ) or with $\mu^+\mu^-\gamma$ events ?

Backup

outline

2021-11-02日讨论：

➤ 束团尺寸/束团能散

- 卷积的话，自变量相同，如果是考虑能散，卷积cross section (u, φ) 时，也得转换成 σu , $\sigma \varphi$;
- 如果是卷积cross section (x, y) 时，考虑 $\sigma s \rightarrow$ 对应的 σx , σy
- 单独分析 θ_e versus ε_0 ：绘制 θ_e 与 ω 图像，改变几组 ε_0 ;
- 分析 $u\theta_0$ versus ε_0 ：绘制 $u\theta_0$ 与 ω 图像，改变几组 ε_0 ;

➤ 对撞角度（非head-on-head）

- $\Delta\alpha = \text{mrad}$, 泰勒展开分析

➤ Layout

- 镜子尺寸：厘米量级
- 散射粒子和主束如果要区分成厘米量级的话，也得是漂移几百公里；所以主束一定得通过镜子，放在磁场前和磁场后是一样的效果；
- 唯一的补偿：我们的mirrow2是一个可以拉伸的装置，测量的话放进去，不测的话拉出来；
- 方案2：激光和电子90度对撞；90度进，90度出。物理要改， $\alpha=180/2 = 90^\circ$ ；意味着截面变小，意味着更长的取数时间。

束流能散

1. 来源

束流能量的精度取决于内在原因和技术因素，例如量子发射、空间电荷效应、Touschek效应、同步辐射等。

2. 意义

束流能量展宽，或称为束流能散，是束流能量的一个重要参量，表征着束流能量的集中性。对束流能散的精确了解可以帮助减小在精确测量中的系统误差。例如，在强子对靠近阈值产生的过程中，能散会影响辐射修正系数、探测效率等参数。对其精确了解可以帮助我们提高这些参数精度。

3. 测量方法

合适。现在加速器上使用的就有很多方法。在束流回旋振荡谱中，存储环的色度会导致同步带峰出现，也就是回旋频率谱上会出现多个峰^[82]。这些峰的幅度与能散有关，可以测它们的相对幅度来得到能散。也可以利用束流回旋运动的测量结果与理论公式比较来得到能散^[83,84]。另外，利用电子和伽马射线的康普顿散射也可以测^[85]。康普顿的反散射边缘由伽马射线能量和电子能量决定，而边缘的宽度则和电子束流能散有关，所以可以测能散。

在北京正负电子对撞机上，通常测量能散的办法是通过对窄共振态的扫描来实现，例如 J/ψ 和 $\psi(2S)$ 。而且能散随能量大体有个平方正比关系，在一个点测量到的能散可以推广到别的能量点上去^[86]。但加速器取数的时间跨度有点长，能量变化大，不同取数时间和取数能量的机器状态可能会不太一样，平方正比关系可能不太合适。所以我们需要寻找新的能散测量方法。

本章我们将介绍两种测量正负电子对撞质心能散的方法。其中一种方法是利用靠近阈值过程的阈值截断效应来测量质心能量的能散 σ_E ，另一种是利用末态特征谱形的分辨来测量束流能散 σ_B 。两种方法测量的能散本质相同，但在对称性正负电子对撞实验中，质心能量是束流能量的 2 倍，所以两者之间的值会相差一个系数 $\sqrt{2}$ ，即 $\sigma_E = \sqrt{2}\sigma_B$ 。

A good approximation for the beam shape in phase space is an ellipse. Any ellipse can be defined by specifying:

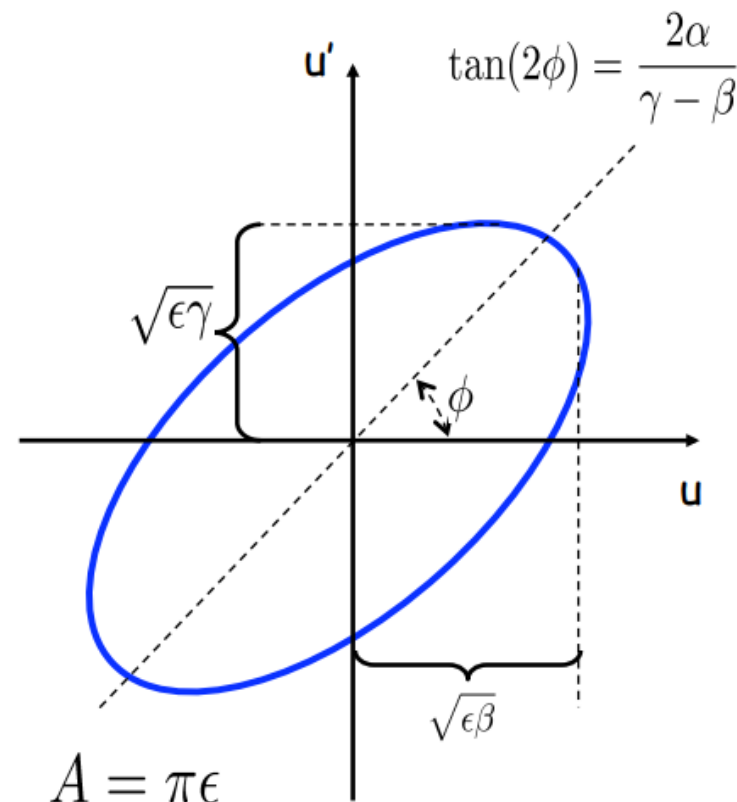
- ✓ Area
- ✓ Shape
- ✓ Orientation

We choose 4 parameters -
3 independent, 1 dependent:

- α - related to beam tilt
- β - related to beam shape and size
- ϵ - related to beam size
- γ - dependent on α and β .

These are the "Twiss
Parameters" (or "Courant-Snyder
Parameters")

Beam Ellipse in Phase Space:



3.1 发射度及能散

束流发射度 ε_i 与能散 σ_e , 将由成像系统测量得到的束流尺寸 σ_i ($i=x, y$ 分别对应束流截面水平、垂直尺寸) 及相关的 Twiss 参数 β_i 、色散函数 η_i , 由公式(11)计算得到。两测量光源点分别为 BS1B01_SP 与 BS1B06_SP, Twiss 参数理论值如表 1 所示。在垂直方向上, 由于两光源点均无色散, 则有 $\sigma_{y1}^2 = \beta_{y1} \varepsilon_y$ 与 $\sigma_{y2}^2 = \beta_{y2} \varepsilon_y$, 由两光源点所测得的垂直尺寸均可直接计算垂直发射度 ε_y , 进行互相验证。在水平方向上, 仅 BS1B06_SP 有色散, 有 $\sigma_{x1}^2 = \beta_{x1} \varepsilon_x$ 与 $\sigma_{x2}^2 = \beta_{x2} \varepsilon_x + (\eta_{x2} \sigma_e)^2$, 由 BS1B01_SP 所测量的 σ_{x1} 可计算发射度 ε_x , 再结合 BS1B06_SP 所测量的 σ_{x2} 可计算能散 σ_e 。即

$$\sigma_i^2 = \beta_i \varepsilon_i + (\eta_i \sigma_e)^2 \quad (11)$$

表 1 BS1B01 与 BS1B06 光源点 Twiss 参数

Table 1 Twiss parameters of BS1B01 and BS1B06 source points

| | β_x (m) | β_y (m) | η_x (m) | η_y (m) |
|-----------|---------------|---------------|--------------|--------------|
| BS1B01_SP | 9.9488 | 5.8821 | 0.0012 | 0 |
| BS1B06_SP | 5.4159 | 5.5444 | 0.1973 | 0 |

3.2 升能过程测量

在升能过程中, 伴随着束流能量的变化, 辐射阻尼效应与量子激发效应会随之变化, 束流发射度与能散也会发生改变。在升能过程初期, 随着辐射阻尼效应的增强, 束流尺寸、发射度与能散等束流参数逐渐减小; 当束流能量达到 3 GeV 时, 这些参数达到最小值, 此后量子激发效应逐渐变得显著; 当达到注入能量 6 GeV 后, 这些参数达到平衡值。

同步光测量系统需要能够监测升能过程中的各束流参数的变化。图 3 为 HEPS 增强器升能降能的周期过程及束流尺寸的测量时序。增强器的重复频率为 1 Hz, 由能量变化曲线可知, 直线束流注入至增强器的过程为 200 ms; 升能过程为 400 ms; 此后到达能量平顶区, 增强器至储存环注入在平顶区完成, 此过程为 200 ms; 降能过程为 200 ms。

[1] 祝德充, 隋艳峰, 岳军会, 彭月梅, 刘佳明, 曹建社. 高能光源增强器束流横向尺寸测量系统设计[J]. 强激光与粒子束, 2021, 33(04):85-89.

曝光时间内的光斑图像, 使用高斯拟合得到的束流尺寸为该段时间内的平均值。因此, 若想获得尽可能接近某能量点下的光斑图像, 需将曝光时间设置得尽可能短。一般来说, CCD 曝光时间在 50 μ s 至 50 ms 内可调节, 需要在保证有效感光的情况下降低曝光时间。

束流在储存环中运动时,有时在横向和纵向会沿平衡轨道作相干振荡,束团沿环运动一圈所作振荡的周期数,通常被称为储存环的 tune 值或 Q 值. 束流的横向(水平或垂直)振荡称为自由振荡,纵向振荡则称为同步振荡或是相振荡. Q 值是储存环的重要参数之一,它的选取对束流的性能影响极大,如果 Q 值的选择不合适,就会造成束流寿命的下降甚至束流的丢失. 另外,加速器的其它一些参数,如包络函数、色品,也要借助于 Q 值测量的数据,通过计算求出. 因此,在加速器运行和机器研究过程中, Q 值测量有着十分重要的意义.

In the design of storage rings there are many similarities with the geometry of optics. In analogy to chromatic aberrations in optics, in particle accelerators a parameter called chromaticity is introduced. In optics rays of different wavelength find a different refraction index in a lens and therefore experience a different focal length. Similarly in a storage ring particles of different momentum see a different focusing strength in the quadrupoles and, as a consequence, have a different betatron oscillation frequency.

We define the chromaticity as the variation of the betatron tune Q with the relative momentum deviation δ ($\delta = \Delta p/p$):

$$Q' = \frac{dQ}{d\delta} . \quad (1)$$

Sometimes the relative chromaticity ξ is used:

$$\xi = \frac{Q'}{Q} . \quad (2)$$

Energy spread measurement

Visible edge width is mostly defined by the energy spread in the electron beam and the γ -detector energy resolution $\frac{\delta r}{r}$:

$$\sigma_\omega \equiv \frac{\delta\omega_{max}}{\omega_{max}} \simeq 2\frac{\delta\varepsilon}{\varepsilon} \oplus \frac{\delta r}{r} (\oplus \frac{\delta\alpha}{\tan(\alpha/2)})$$

One can derive energy spread in the electron beam from σ_ω :

$$\sigma_\varepsilon \equiv \frac{\delta\varepsilon}{\varepsilon} \simeq \frac{1}{2}\sqrt{\sigma_\omega^2 - \sigma_r^2}$$

Energy spread measurement accuracy is thus given by:

$$\frac{\Delta\sigma_\varepsilon}{\sigma_\varepsilon} \simeq \frac{\sigma_\omega d\sigma_\omega \oplus \sigma_r d\sigma_r}{\sigma_\omega^2 - \sigma_r^2}$$

能散问题

Table 4.1.1: CEPC parameters

| | Higgs | W | Z (3T) | Z (2T) |
|---|----------------|------------------|-------------------|-------------|
| Number of IPs | | 2 | | |
| Beam energy (GeV) | 120 | 80 | 45.5 | |
| Circumference (km) | | 100 | | |
| Synchrotron radiation loss/turn (GeV) | 1.73 | 0.34 | 0.036 | |
| Crossing angle at IP (mrad) | | 16.5 × 2 | | |
| Piwnski angle | 3.48 | 7.0 | 23.8 | |
| Particles /bunch $N_e (10^{10})$ | 15.0 | 12.0 | 8.0 | |
| Bunch number | 242 | 1524 | 12000 (10% gap) | |
| Bunch spacing (ns) | 680 | 210 | 25 | |
| Beam current (μA) | 17.4 | 87.9 | 461.0 | |
| 同步辐射能散 $[\sigma_{\delta,\text{SR}}]$ | | % | | 0.13 |
| 束束韧致辐射能散 $[\sigma_{\delta,\text{BS}}]$ | | % | | 0.09 |
| 总能散 $[\sigma_{\delta,\text{tot}}]$ | | % | | 0.16 |
| Beam size at IP $\sigma_x/\sigma_y (\mu\text{m})$ | 20.9/0.06 | 15.9/0.049 | 6.0/0.078 | 6.0/0.04 |
| Beam-beam parameters ξ_x/ξ_y | 0.018/0.109 | 0.013/0.123 | 0.004/0.06 | 0.004/0.079 |
| RF voltage $V_{RF} (\text{GV})$ | 2.17 | 0.47 | 0.10 | |
| RF frequency $f_{RF} (\text{MHz})$ | | 650 | | |
| Harmonic number | | 216816 | | |
| Natural bunch length $\sigma_z (\text{mm})$ | 2.72 | 2.98 | 2.42 | |
| Bunch length $\sigma_z (\text{mm})$ | 4.4 | 5.9 | 8.5 | |
| Damping time $\tau_x/\tau_y/\tau_E (\text{ms})$ | 46.5/46.5/23.5 | 156.4/156.4/74.5 | 849.5/849.5/425.0 | |
| Natural Chromaticity | -468/-1161 | -468/-1161 | -491/-1161 | -513/-1594 |
| Betatron tune v_x/v_y | | 363.10 / 365.22 | | |
| Synchrotron tune v_s | 0.065 | 0.040 | 0.028 | |
| HOM power/cavity (2 cell) (kw) | 0.46 | 0.75 | 1.94 | |
| Natural energy spread (%) | 0.100 | 0.066 | 0.038 | |
| Energy spread (%) | 0.134 | 0.098 | 0.080 | |
| Energy acceptance requirement (%) | 1.35 | 0.90 | 0.49 | |

